



This is a repository copy of *Analysis and sources identification of atmospheric PM10 and its cation and anion contents in Makkah, Saudi Arabia.*

White Rose Research Online URL for this paper:
<https://eprints.whiterose.ac.uk/182340/>

Version: Published Version

Article:

Habeebullah, T.M., Munir, S. orcid.org/0000-0002-7163-2107, Zeb, J. et al. (1 more author) (2022) Analysis and sources identification of atmospheric PM10 and its cation and anion contents in Makkah, Saudi Arabia. *Atmosphere*, 13 (1). 87.

<https://doi.org/10.3390/atmos13010087>

Reuse

This article is distributed under the terms of the Creative Commons Attribution (CC BY) licence. This licence allows you to distribute, remix, tweak, and build upon the work, even commercially, as long as you credit the authors for the original work. More information and the full terms of the licence here:
<https://creativecommons.org/licenses/>

Takedown


If you consider content in White Rose Research Online to be in breach of UK law, please notify us by emailing eprints@whiterose.ac.uk including the URL of the record and the reason for the withdrawal request.



eprints@whiterose.ac.uk
<https://eprints.whiterose.ac.uk/>

Article

Analysis and Sources Identification of Atmospheric PM₁₀ and Its Cation and Anion Contents in Makkah, Saudi Arabia

Turki M. Habeebullah ¹, Said Munir ^{2,*} , Jahan Zeb ¹ and Essam A. Morsy ¹

¹ Department of Environmental and Health Research, The Custodian of the Holy Two Mosques Institute for Hajj and Umrah Research, Umm Al Qura University, Makkah 21955, Saudi Arabia; tmhabeebullah@uqu.edu.sa (T.M.H.); jzhabib@uqu.edu.sa (J.Z.); eamibrahim@uqu.edu.sa (E.A.M.)

² Department of Civil and Structural Engineering, University of Sheffield, Sheffield S1 3JD, UK

* Correspondence: smunir2@sheffield.ac.uk; Tel.: +44-7986001328

Abstract: In this paper, atmospheric water-soluble cation and anion contents of PM₁₀ are analysed in Makkah, Saudi Arabia. PM₁₀ samples were collected at five sites for a whole year. PM₁₀ concentrations ($\mu\text{g}/\text{m}^3$) ranged from 82.11 to 739.61 at Aziziyah, 65.37 to 421.71 at Sanaiyah, 25.20 to 466.60 at Misfalah, 52.56 to 507.23 at Abdeyah, and 40.91 to 471.99 at Askan. Both daily and annual averaged PM₁₀ concentrations exceeded WHO and Saudi Arabia national air quality limits. Daily averaged PM₁₀ concentration exceeded the national air quality limits of $340 \mu\text{g}/\text{m}^3$, 32% of the time at Aziziyah, 8% of the time at Sanaiyah, and 6% of the time at the other three sites. On average, the cations and anions made a 37.81% contribution to the PM₁₀ concentrations. SO_4^{2-} , NO_3^- , Ca^{2+} , Na^+ , and Cl^- contributed 50.25%, 16.43%, 12.11%, 11.12%, and 8.70% to the total ion concentrations, respectively. The minor ions (F^- , Br^- , Mg^{2+} , NO_2^- , and PO_4^{3-}) contributed just over 1% to the ion mass. Four principal components explained 89% variations in PM₁₀ concentrations. Four major emission sources were identified: (a) Road traffic, including emission from the exhaust, wear-and-tear, and the resuspension of dust particles (F^- , SO_4^{2-} , NO_3^- , Ca^{2+} , Na^+ , Mg^+ , Br^- , Cl^- , NO_2^- , PO_4^{3-}); (b) Mineral dust (Cl^- , F^- , Na^+ , Ca^{2+} , Mg^{2+} , PO_4^{3-}); (c) Industries and construction–demolition work (F^- , SO_4^{2-} , Ca^{2+} , Mg^{2+}); and (d) Seaspray and marine aerosols (Cl^- , Br^- , Mg^{2+} , Na^+). Future work would include an analysis of the metal contents of PM₁₀ and their spatiotemporal variability in Makkah.

Keywords: cations; anions; particulate matter (PM₁₀); air pollution; Makkah; source apportionment; PCA



Citation: Habeebullah, T.M.; Munir, S.; Zeb, J.; Morsy, E.A. Analysis and Sources Identification of Atmospheric PM₁₀ and Its Cation and Anion Contents in Makkah, Saudi Arabia. *Atmosphere* **2022**, *13*, 87. <https://doi.org/10.3390/atmos13010087>

Academic Editor:
Liudmila Golobokova

Received: 20 November 2021
Accepted: 3 January 2022
Published: 6 January 2022

Publisher's Note: MDPI stays neutral with regard to jurisdictional claims in published maps and institutional affiliations.



Copyright: © 2022 by the authors. Licensee MDPI, Basel, Switzerland. This article is an open access article distributed under the terms and conditions of the Creative Commons Attribution (CC BY) license (<https://creativecommons.org/licenses/by/4.0/>).

1. Introduction

In recent decades, air pollution has been one of the most important health concerns for humans. Both human health and the ecosystem are facing considerable damage due to the high levels of air pollution in urban areas [1]. As per the World Health Organisation (WHO) evaluation, ambient air pollution was responsible for 4.2 million deaths worldwide in 2016. Globally, 91% of humans are living in areas where air pollutants exceed WHO air quality limits. According to the WHO [2], mortality due to poor air quality could be reduced by 12.7% if the average PM_{2.5} and PM₁₀ levels were decreased from $35 \mu\text{g}/\text{m}^3$ to $10 \mu\text{g}/\text{m}^3$ and $70 \mu\text{g}/\text{m}^3$ to $20 \mu\text{g}/\text{m}^3$, respectively. According to the World Bank, air pollution is the fourth largest reason for human mortality globally [3]. Criteria pollutants, viz., CO, O₃, particulate matter (PM₁₀ and PM_{2.5}), NO₂, and SO₂, are responsible for serious cardiovascular and respiratory diseases [4].

Air pollution is the cost of rapid industrialisation and urbanisation in the world [5], including in Middle Eastern countries such as Saudi Arabia. Investors are attracted by allocating more land for industries, refineries, and shopping centres, which are the cause of an increase in stationary and mobile sources of air pollution. Government guidelines and regulations are implemented for cutting emissions and improving air quality in Makkah; however, further work is required to fully understand emission sources [6]. Makkah city

has unique characteristics in terms of geographical location, meteorological conditions, and religious importance in the Muslim world. It is the holiest city for Muslims, and millions of pilgrims visit the city every year during the month of Hajj and Ramadan. Approximately 2.5 million pilgrims performed Hajj in 2019 [7]. Visitors come to Makkah not only from inside Saudi Arabia but also from other countries throughout the world. The mass movement of humans through vehicles, the usage of air conditioners, cooking, and consumption of other resources put an extra burden on the city system and negatively affect the city's natural environment and air quality [8,9]. The situation is made worst by the dry and hot climatic conditions and frequent dust storms, which increase background PM concentrations in the atmosphere [10,11].

A study on the source apportionment and elemental composition of atmospheric total suspended particles (TSP) along the Red Sea coast in Saudi Arabia revealed that the concentrations of TSP at a stationary air quality monitoring site and an off-shore mobile site were $125 \mu\text{g}/\text{m}^3$ and $108 \mu\text{g}/\text{m}^3$, respectively [12], which is much lower compared to the present study and compared to Habeebullah [13]. Crustal materials and oil combustion were identified as the major sources of TSP [12]. A 12-months study [11] in Makkah on the concentrations and source apportionment of $\text{PM}_{2.5}$ reported that $\text{PM}_{2.5}$ demonstrated significant seasonal variability in the city. The levels of $\text{PM}_{2.5}$ ($\mu\text{g}/\text{m}^3$) were 113 in spring, 88.3 in summer, 67.8 in fall, and 67.6 in winter [7]. Employing positive matrix Factorisation (PMF), four major sources were identified, namely, vehicular emission, industrial mixed dust, soil/earth crust, and fossil fuel combustion [11]. Several other studies were carried out in Western Saudi Arabia on source apportionment and elemental composition of $\text{PM}_{2.5}$ and PM_{10} [6,11–13], which revealed that water-soluble ions were also present in a significant amount along with metal and non-metal elements. Ionic components of PM have their own importance and are related to acid rain, acidity, and the harmfulness of pollutants. The literature [13–16] shows that water-soluble ions in PM act differently in different pollution sources and in different climatic conditions. Ionic analysis not only characterises the nature and composition of PM but also reveals the scientific explanation of the formation and transmission mechanisms of PM [15–19].

Limited air quality studies are carried out in this region due to data limitations, particularly for particulate matter (e.g., PM_{10}) and its constituents. There is a need for further studies to characterise PM_{10} and analyse its chemical composition. PM_{10} samples were collected, analysed for ion contents in the laboratory, and statistically analysed employing various statistical techniques. The main focus is on the quantitative analysis of water-soluble ionic species in PM_{10} in Makkah city, Saudi Arabia. The aim is to quantify the percentage contribution of various cations and anions to the PM_{10} concentrations. The study also aims to identify the major sources of PM_{10} emissions in Makkah by performing principal component analysis (PCA). The study will help understand the causes of PM_{10} pollution in Makkah, which will be helpful in preparing a strategy for air quality management and control in Makkah.

2. Materials and Methods

2.1. Description of the Monitoring Sites

The sites for PM_{10} samples collection were selected to represent the major activities in Makkah (Figure 1). The Holy City of Makkah is one of the most densely populated cities in Saudi Arabia, and according to the general authority for statistics of the Kingdom of Saudi Arabia [20], its population is more than 8.5 million, with a growth rate of 1.8%. In addition, every year, millions of Muslims from all over the world visit Makkah to perform Hajj and Umrah. Due to its hot arid nature, the annual mean temperature in Makkah is 31.42°C , and the maximum temperature reaches over 55°C in hot months of the year [21]. Its climate is dry, receiving very little rain every year. The city is expanding rapidly, and different towns around Makkah share its characteristics of multistorey buildings, fewer or no trees except date palms, and being busy all year round in terms of national and international visitors. However, in terms of road traffic, the central region of Makkah is busier than the

surrounding outskirts. For example, Misfalah and Aziziyah are considered the busiest, whereas Abdeyah and Sanaiyah are relatively quieter. Samples were collected at residential, central urban, industrial, traffic, and background areas. PM₁₀ samples were collected at five monitoring sites, namely, Aziziyah (urban traffic area), Misfalah (central urban area), Sanaiyah (industrial area), Askan (residential area), and Abdeyah (background area).

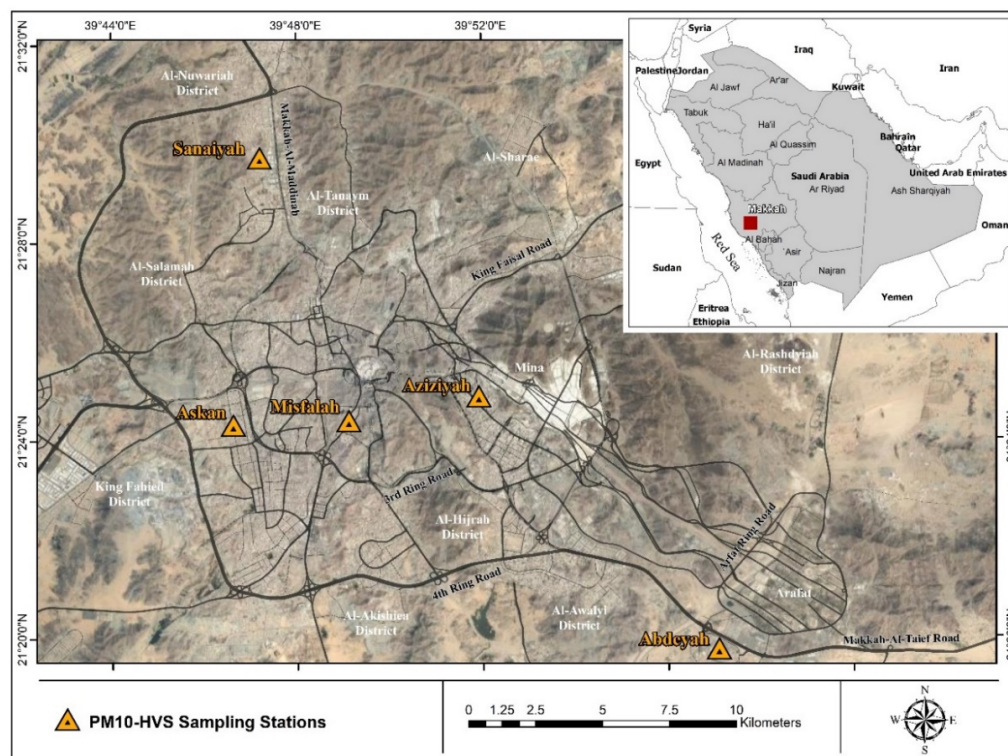


Figure 1. Location map of the sampling stations of PM₁₀-HVS in Makkah.

Aziziyah is considered an urban traffic site, which means the pollutant emissions predominantly come from road traffic. However, Aziziyah district is also famous for commercial activities such as shopping centres and public services such as restaurants, libraries, and pharmacies. Misfalah is one of the historical districts of Makkah and is so named due to its geographical level descending from the Grand Mosque. Major traffic roads in Misfalah district are the second ring road and Umm Al-Qura Road in the north, the third ring road in the south, Prince Mutaib bin Abdulaziz Road in the east, and the third ring road in the west. Similar to Aziziyah, the major emission source here is road traffic. Sanaiyah (Al-Taneem) is one of the industrial districts of Makkah. Al-Taneem district, in addition, to other industrial activities, has the electrical power station of Makkah. In Sanaiyah, the major anthropogenic emission sources are industrial units and road traffic. Askan is one of the residential districts of Makkah, belonging to the municipality of Al-Shawqiyyah. In terms of road traffic, it is quieter than Aziziyah and Misfalah and probably busier than Abdeyah. It is considered one of the poor areas in Makkah. Abdeyah is one of the new districts of Makkah and is in the southeast of the city of Makkah. The new campus of Umm al Qura University is the major landmark. It is situated outside the main city of Makkah and therefore is not as congested as Aziziyah and Misfalah. Its busiest day of the year is the day of Arafah (9th Zulhijjah) when pilgrims spend the whole day in Arafat and then return to Muzdalifah after the sun sets.

2.2. Sample Collection

PM₁₀ samples were collected on hi-volume glass fibre filters (8 × 10 inches, Grade G 653, Whatman), using a high-volume air sampler (Staplex), with inlet collection effi-

ciency of a cut-point of 9.7 microns over a wind speed of 0 to 36 km/hr and flow rate of 1.13 m³/min. A sampling calendar was prepared to cover all days of the week throughout the year to focus on all activities in Makkah by a period interval of six days. Filters were changed strictly from 9:00 to 10:00 a.m. Sample collection time was from 8 March 2020 to 9 March 2021. However, due to the strict COVID-19 lockdown in Makkah, the collection of samples was suspended at every sampling site during the period from 7 April 2020 to 31 May 2020. Therefore, data are missing for April and May 2020. The glass fibre filters were put into an oven (LDO-060E, Lab Tech) at 300 °C for 5 h to remove moisture and organic contaminants. Then, the filters were kept in a desiccator at room temperature for the next 24 h and weighed by an analytical balance (ABT 120-5DM, Kern) until the constant mass was observed. Finally, the filters were sealed in polyethylene bags until their analysis [22].

2.3. Analysis of PM₁₀ Samples

2.3.1. Gravimetric Analysis

After a 24 h sampling period, the filters were transported to the laboratory in polyethylene bags, where the filters were again weighed (until constant weighed observed) in the same analytical balance for the determination of exact deposited mass. After post weighing, filters were cut into four equal pieces for further chemical analysis and stored in the refrigerator at 4 °C [23].

PM₁₀ concentrations were calculated by the gravimetric method. Pre and post weights of the filter paper along with the total volume of air passed were used in calculations. The following equation (Equation (1)) was used for the calculation [24]:

$$PM_{10} = \frac{(W_f - W_i) \times 10^6}{V} \quad (1)$$

where,

PM₁₀ = concentrations of PM₁₀ particles on sample filters in µg/m³.

W_f = post-weight of PM₁₀ filters in g.

W_i = pre-weight of PM₁₀ filters in g.

V = total volume of air passing through PM₁₀ filters in m³.

2.3.2. Analysis of Water-Soluble Ions

After the gravimetric analysis of PM₁₀, the sample filter papers were cut into four equal parts. One-fourth of every filter was reserved for ionic analysis, which were fluoride (F⁻), chloride (Cl⁻), nitrite (NO₂⁻), bromide (Br⁻), nitrate (NO₃⁻), sulphate (SO₄²⁻), phosphate (PO₄³⁻), sodium (Na⁺), calcium (Ca²⁺), and magnesium (Mg²⁺). A quarter ($\frac{1}{4}$) of each filter was shredded into a 50 mL conical flask, already containing 25 mL of deionised distilled water with a resistivity of 18 Ωcm. In order to extract the ions from sample filter paper into deionised distilled water, a conical flask was ultrasonicated for 1 h in an ultrasonic bath (ATM40-28LCD, Ovan). After sonication, the sample was filtered through a 0.45 µm pore size membrane filter (CHROMAFIL, CA-45/25 (S), Macherey-Nagel), to remove the undissolved particles, and the extract was stored in a refrigerator at 4 °C [18].

The sample extract was analysed for the determination of ion concentrations in PM₁₀ samples using Ion Chromatography (850 Professional, Metrohm). Nitric acid (3.2 mM) and sodium carbonate (1.8 mM) were used as cationic and anionic solvents, respectively. The flow rate was maintained at 0.7 mL/min, whereas the injection volume of both cationic and anionic solvents was 10 µL [23]. All required measures were adopted for quality assurance, including triplicate samples and blank calibrations. Samples were analysed in triplicate, and their mean values were reported. The detection limit (ppm) was 0.001 for fluoride and phosphate, 0.002 for sodium and magnesium, and 0.005 for chloride, nitrite, bromide, nitrate, and calcium.

2.4. Statistical Analysis

The cation and anion data were analysed using the R programming language [25] and two of its packages, 'openair' [26] and 'ggplot2' [27]. Correlation analysis was performed to investigate the linear relationship between different ions. A correlation plot was developed in the openair package [26] using its function 'corPlot'. Principal component analysis (PCA) was performed using data of all ions from all sites. Furthermore, PCA was also performed for each site. PCA enables us to identify groups of ions that are similar and group them into different principal components (PC). PCA is an exploratory data analysis technique that reduces the dimensionality of a dataset with a large number of variables. PCA increases interpretability and minimises information loss of the dataset by producing uncorrelated PC. The Eigenvalue is the standard deviation of each PC, which describes the variance of the PC. The Eigenvector with the highest Eigenvalue is the first PC. Each PC explains a certain percentage of the total variance in the dataset. For more information on PCA and its uses, readers are referred to Park and Dam [28], Zuska et al. [29], and Cesari et al. [30].

3. Results and Discussion

The concentrations of cations, anions and PM₁₀ ($\mu\text{g}/\text{m}^3$) at the five monitoring sites in Makkah are depicted in Figure 2. Mean PM₁₀ concentrations ($\mu\text{g}/\text{m}^3$) was 303.18 (ranging from 82.11 to 739.61) at the Aziziyah site, which was the highest among the five sites. Mean PM₁₀ concentrations ($\mu\text{g}/\text{m}^3$) were 154.97 (ranging from 65.37 to 421.71) at Sanaiyah, 219.41 (ranging from 25.20 to 466.60) at Misfalah, 177.99 (ranging from 52.56 to 507.23) at Abdeyah, and 164.53 (ranging from 40.91 to 471.99) at Askan. The air quality standard set by the Presidency of Meteorology and Environment (PME) of Saudi Arabia for PM₁₀ is 340 ($\mu\text{g}/\text{m}^3$) for 24 h average and 80 ($\mu\text{g}/\text{m}^3$) for an annual average [31]. The PM₁₀ data presented in Figure 2 is based on 24 h sampling periods, which shows that maximum concentrations at all five sites are above the 24 h air quality limit. The 24 h averaged PM₁₀ concentrations exceeded the PME limits 32% of the time at Aziziyah, 8% of the time at Sanaiyah, and 6% of the time at each Misfalah, Askan, and Abdeyah site (Figure 2d). The annual average of PM₁₀ exceeded the annual air quality limit of 80 $\mu\text{g}/\text{m}^3$ at all sites. This probably shows that PM₁₀ levels are a cause of concern in Makkah. Such high levels of PM₁₀ have been previously reported by several researchers in Saudi Arabia. Researchers who used data from continuous reference air quality monitoring stations have also reported such high PM₁₀ levels in Makkah. For example, Mohammed et al. [32] reported that during the Hajj (Pilgrimage) period from 8th to 12th Zulhijjah (the 12th month of the Islamic calendar) in 2011, PM₁₀ levels ranged from 405 to 527 $\mu\text{g}/\text{m}^3$. Furthermore, Habeebullah [13] reported that average levels of TSP, PM₁₀ and PM_{2.5} were 366.38, 233.38 and 143.49 $\mu\text{g}/\text{m}^3$, respectively, during 2013 in Makkah. Several other researchers have also reported such high levels of PM in Makkah [8,9,33,34]. Therefore, it is expected to observe such high levels of PM₁₀ in Makkah, Saudi Arabia. High levels of PM₁₀ in Makkah are attributed to the geographical and meteorological conditions of the regions. Makkah experiences dry and hot climatic conditions and is surrounded by large sandy deserts [10,11]. Sand and dust storms are frequent in Saudi Arabia. These geographical and climatic conditions add positively to the levels of particulate pollution in Makkah [10,11]. Furthermore, the city is expanding rapidly, where large-scale construction-and-demolition projects are taking place that add to the atmospheric PM load [9]. Aziziyah is famous for heavy road traffic, and therefore, frequent traffic congestion during the busy hours of the day is common, which causes pollution episodes by emissions from the tailpipes, wears-and-tears, and resuspension of dust on roadsides. This makes Aziziyah one of the most polluted sites in Makkah (Figure 2).

Levels of PM₁₀ and cations and anions are depicted in Figure 2, which shows that not only the levels of PM₁₀ but also the levels of cations and anions are higher at the Aziziyah site. Cations and anions are divided into two subgroups based on their levels (Figure 2). These subgroups are referred to as major and minor ions in this study. The major ions are chloride (Cl^-), sodium (Na^+), calcium (Ca^{2+}), nitrate (NO_3^-), and sulphate

(SO_4^{2+}), in ascending order of their levels in PM_{10} . Among the major ions, Cl^- has the lowest levels ranging from 4.73 to 10.21 ($\mu\text{g}/\text{m}^3$), and SO_4^{2-} has the highest levels ranging from 30.75 to 52.32 ($\mu\text{g}/\text{m}^3$). The minor ions are nitrite (NO_2^-), bromide (Br^-), phosphate (PO_4^{3-}), fluoride (F^-), and magnesium (Mg^{2+}). NO_2^- has the lowest levels ranging from 0.01 to 0.02 ($\mu\text{g}/\text{m}^3$), whereas Mg^{2+} has the highest level ranging from 0.36 to 0.59 ($\mu\text{g}/\text{m}^3$). Minor ions are all in fractions and are presented in a separate panel of Figure 2. Mohammed et al. [33] analysed various cations and anions in PM_{10} (along with $\text{PM}_{2.5}$ and total suspended particulates) in Makkah and reported that NO_3^- and SO_4^{2-} were the most dominant anions in PM_{10} . In the current study, the average concentrations of SO_4^{2-} and NO_3^- in PM_{10} were 40.35 and 17.26 ($\mu\text{g}/\text{m}^3$), respectively, whereas according to Mohammed et al. [33], SO_4^{2-} and NO_3^- levels were 21.8 and 5.5 $\mu\text{g}/\text{m}^3$, respectively. Both studies show that SO_4^{2-} levels are higher in PM_{10} than the NO_3^- levels. The levels of both NO_3^- and SO_4^{2-} reported in the current study are higher than those reported by Mohammed et al. [33]. Changes in the levels and proportion of ions in PM_{10} are expected as pollutant levels, and emission sources may change both in time and space. It should be noted that Mohammed et al. [32] had collected PM_{10} samples at a single rural site in Mina during the Hajj period, whereas in this study, samples were collected from five sites, mostly urban, which explain why the levels are higher in this study. Furthermore, in the present study, we used data for a whole year, whereas Mohammed et al. [32] collected samples for just a single week.

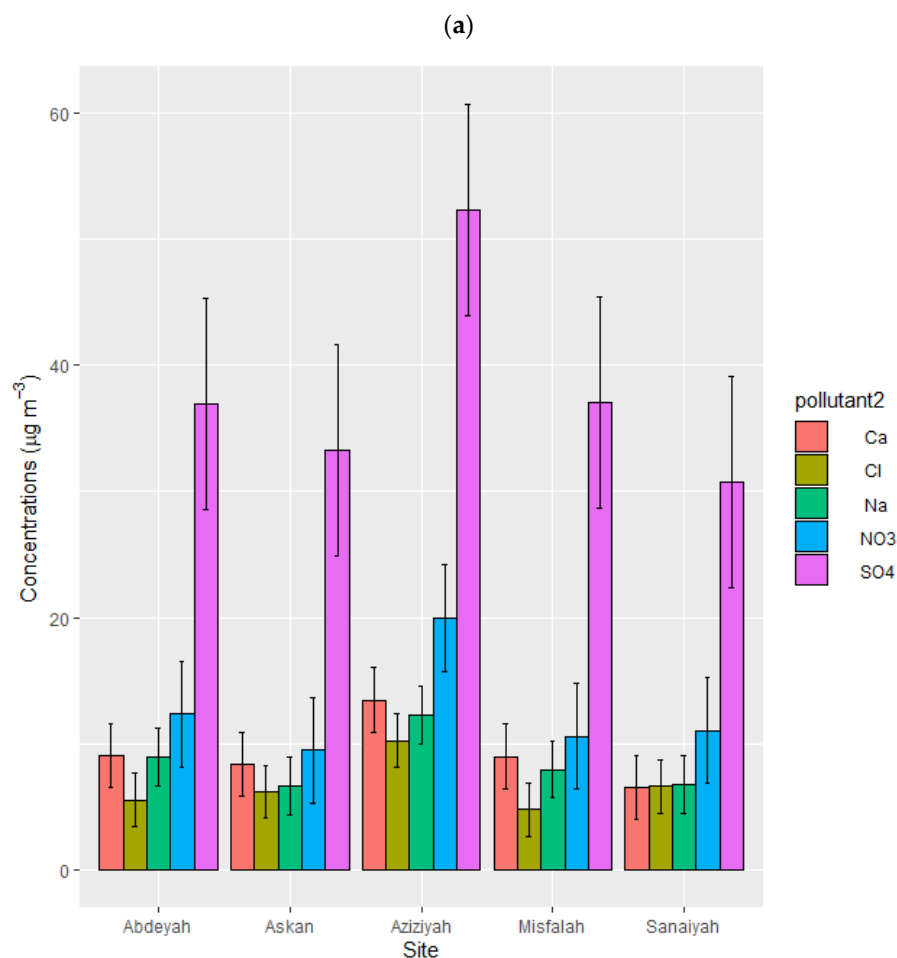
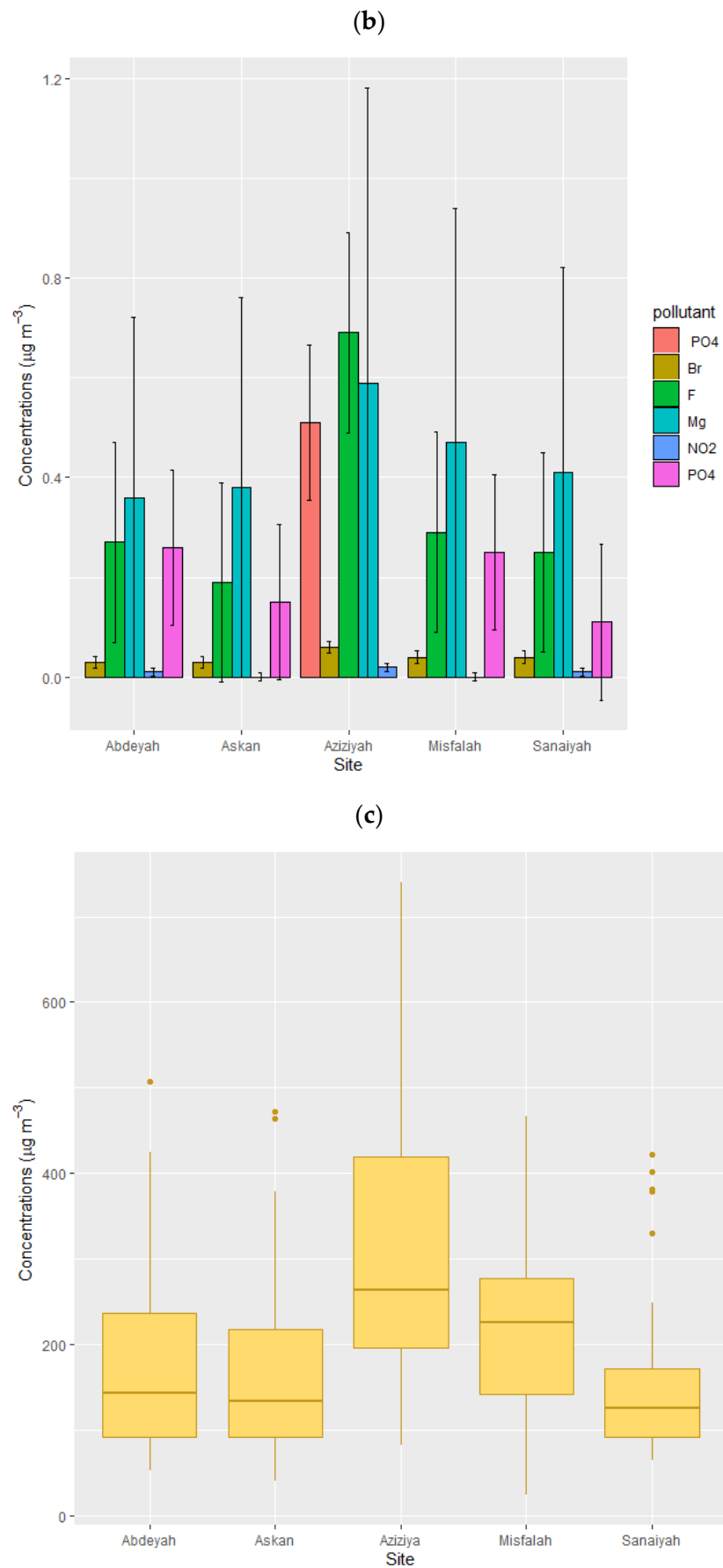


Figure 2. Cont.



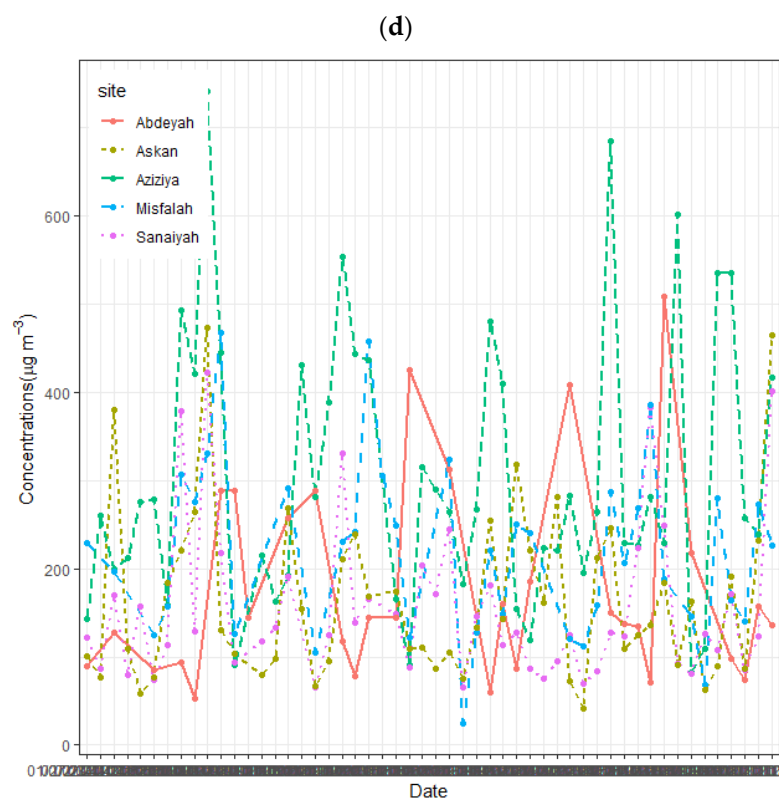


Figure 2. Comparing the levels of different ions using bar plots (a,b), PM_{10} concentrations using box plots (c), and time series of PM_{10} (d) at different sites in Makkah. The lower end of the box shows 1st quartile, the upper end of the box shows 3rd quartile, and the horizontal line in the middle of the box shows the median of the data. The top and lower ends of the vertical orange line show maximum and minimum values, respectively, whereas the dots above the vertical line shows outliers.

Habeebullah [13] analysed PM_{10} samples collected from August 2012 to September 2013 at four sites in Makkah and studied the composition of PM_{10} focusing on heavy metals, and cations and anions. Habeebullah [13], in addition to heavy metals, namely Lead (Pb), Nickel (Ni), Cadmium (Cd), Chromium (Cr), Vanadium (V), Arsenic (As), Mercury (Hg), and Aluminium (Al), quantified the levels of cations and anions which were Cl^- , Br^- , F^- , NH_4^+ , PO_4^{3-} , SO_4^{2-} , NO_3^- , and NO_2^- . According to Habeebullah [13] NO_3^- and SO_4^{2-} were the most abundant ions in PM_{10} . NO_3^- content was 39.79% and SO_4^{2-} content was 17.02% in PM_{10} . Habeebullah [13] found that NO_3^- levels were higher than SO_4^{2-} levels, in contrast to the current study and Mohammed et al. [32]. This could be due to temporal variations or spatial variations, or both, as these studies did not use simultaneously collected data from the same sites. Nayebare et al. [11] analysed $PM_{2.5}$ concentration and its chemical composition in Makkah from February 2014 to January 2015. They found that 24 h averaged $PM_{2.5}$ concentrations exceeded WHO and Saudi Arabia national air quality guidelines, and according to the air quality index, air quality was classified as ‘unhealthy to hazardous’. They also reported that $PM_{2.5}$ levels demonstrated significant temporal variations, and its levels varied from season to season. $PM_{2.5}$ concentrations ($\mu g/m^3$) were 113.0, 88.3, 67.8, and 67.6 in spring, summer, fall, and winter, respectively. They analysed the composition of $PM_{2.5}$ but mainly focused on trace elements and did not consider the levels of NO_3^- , SO_4^{2-} , NH_4^+ , PO_4^{3-} , and other ion species. Therefore, no comparison could be made between the levels of cations and anions analysed in Nayebare et al. [11] and the current study. Similarly, Khodeir et al. [14] collected PM_{10} and $PM_{2.5}$ samples for several weeks between June and September 2011 at seven sites in Jeddah. According to their analysis, the averaged PM_{10} and $PM_{2.5}$ concentrations ($\mu g/m^3$) were 87.3 and 28.4, respectively, with significant spatiotemporal variability. Concentrations of both PM_{10} and $PM_{2.5}$ exceeded

the daily air quality guidelines of the WHO and the European Union. Khodeir et al. [14] analysed PM samples for 33 elements; however, the cations and anions considered in the current study were mostly not considered. Therefore, a comparison between the levels of cations and anions was not possible.

The percentage contribution of cations and anions to the PM₁₀ concentration was calculated (Table 1) for each site. To do so, the concentrations of all ions were summed up and converted to percent contribution using the formula given below (Equation (2)):

$$\text{Percent contribution} = (\text{Sum of ion conc.}/\text{PM}_{10} \text{ conc.}) \times 100 \quad (2)$$

Table 1. Sum of ion concentrations ($\mu\text{g}/\text{m}^3$) and their percent contribution to PM₁₀ concentrations ($\mu\text{g}/\text{m}^3$) at different monitoring sites.

Site	PM ₁₀ Conc.	Ions Conc.	% Contribution
Aziziyah	303.18 ± 169.00	110.03 ± 31.61	36.29 ± 5.39
Sanaiyah	155.55 ± 24.57	62.42 ± 6.49	40.13 ± 8.81
Misfalah	219.7 ± 7.89	70.28 ± 7.69	31.99 ± 3.41
Abdeyah	177.99 ± 21.67	73.69 ± 6.03	41.40 ± 4.31
Askan	164.53 ± 81.53	64.60 ± 17.60	39.26 ± 4.07
average	204.19 ± 60.93	76.20 ± 13.89	37.81 ± 5.20

On average, the cations and anions analysed in this study made a 37.81% contribution to the PM₁₀ concentrations. The percentage proportion of ions to PM₁₀ varied from site to site and ranged from 31.99% (Misfalah) to 41.40% (Abdeyah) (Table 1). This meant that approximately 58% to 68% of PM₁₀ consisted of other components, including organic chemicals, metals, and soil or dust particles. On average SO₄²⁻, NO₃⁻, Ca²⁺, Na⁺, and Cl⁻ contributed 50.25%, 16.43%, 12.11%, 11.12%, and 8.70%, respectively, to the total ion mass. The percent contribution of individual ions to the total mass of ions varied from site to site; however, the order was the same, which was SO₄²⁻ > NO₃⁻ > Ca²⁺ > Na⁺ > Cl⁻ (Table 2). The minor ions contributed just over 1% to the ion mass.

Table 2. Percent contribution of each ion to the total ion mass at different monitoring sites.

Ions	Aziziyah	Sanaiyah	Misfalah	Abdeyah	Askan	Average
F ⁻	0.63 ± 0.47	0.40 ± 0.01	0.41 ± 0.20	0.37 ± 0.07	0.29 ± 0.02	0.42 ± 0.15
Cl ⁻	9.28 ± 8.26	10.51 ± 0.54	6.73 ± 0.93	7.46 ± 0.26	9.52 ± 1.58	8.70 ± 2.31
NO ₂ ⁻	0.02 ± 0.01	0.02 ± 0.01	0.01 ± 0.01	0.01 ± 0.01	0.01 ± 0.01	0.01 ± 0.01
Br ⁻	0.05 ± 0.03	0.06 ± 0.01	0.06 ± 0.04	0.04 ± 0.01	0.05 ± 0.01	0.05 ± 0.02
NO ₃ ⁻	18.13 ± 5.11	17.67 ± 6.40	15.03 ± 0.91	16.75 ± 1.49	14.60 ± 2.59	16.43 ± 3.30
PO ₄ ³⁻	0.46 ± 0.19	0.18 ± 0.03	0.36 ± 0.04	0.35 ± 0.05	0.23 ± 0.01	0.32 ± 0.06
SO ₄ ²⁻	47.55 ± 10.23	49.26 ± 0.30	52.73 ± 2.19	50.13 ± 1.54	51.56 ± 10.72	50.25 ± 5.00
Na ⁺	11.12 ± 3.02	10.78 ± 0.40	11.28 ± 5.62	12.16 ± 4.55	10.28 ± 0.16	11.12 ± 2.75
Ca ²⁺	12.22 ± 4.21	10.46 ± 0.35	12.73 ± 1.79	12.24 ± 1.64	12.88 ± 2.79	12.11 ± 2.16
Mg ²⁺	0.54 ± 0.09	0.66 ± 0.05	0.67 ± 0.06	0.49 ± 0.03	0.59 ± 0.07	0.59 ± 0.06

To show how the levels of various ions have changed in both space and time, monthly average concentrations of PM₁₀ (top-panel), major ions (middle panel) and minor ions (lower panel) are depicted in Figure 3, which shows significant spatiotemporal variability in PM₁₀ and its constituents within Makkah caused by changes in emission sources and microlevel meteorological conditions. It should be noted that due to the COVID-19 lockdown in Saudi Arabia, it was not possible to collect the samples from 7 April to 31 May 2020; therefore, data are not shown in Figure 3 for these months. It is also important

to mention that in 2020 Hajj was cancelled in 2020. It was supposed to occur in August, otherwise, pollutant concentrations would have been much higher in August 2020. The highest monthly concentrations of PM_{10} and ions were observed in September in Aziziyah (Figure 3). However, the temporal pattern was not the same at different monitoring sites. The COVID-19 lockdown not only affected air pollutant emissions from road traffic but also affected the resuspension of dust particles on roadsides, emissions from factories, and dust generated by construction and demolition activities. Changes in the emission activities resulted in significant effects on air pollution levels. Morsy et al. [35] analysed air quality data from six monitoring sites and assessed the effect of the COVID-19 lockdown on the levels of different air pollutants, including PM_{10} in Makkah. They reported that during the lockdown period, the levels of PM_{10} decreased by 30% compared to the pre-lockdown period. This contributed to a reduction in the levels of road traffic in Makkah; however, the lockdown also affected other activities, including the operation of factories, international travel, the closure of markets, and the closure of Al-Haram (the Holy Grand Mosque in Makkah). Morsy et al. [35] showed that the levels of PM_{10} and other gaseous pollutants decreased during the lockdown period; however, it should not affect the results of this because samples were not analysed in April and May.

A histogram (Figure 4, upper panel) of wind speed during 2020 shows that most of the time wind speed (m/s) was 0.5–1.0 and 1.0–1.5, which had a frequency of 1695 and 1816, respectively. The maximum wind speed was 6 m/s; however, the frequency of wind speed greater 3 m/s was very low. Wind speed (m/s) from 3.0–3.5, 3.5–4.0, and 4.0–6.0 had a frequency of 29, 20, and 7, respectively. Figure 4 (middle panel), showing the polar frequency plot, demonstrates the highest frequency in the northwest direction (northwesterly wind). The effect of wind speed and wind direction depends on the distance and direction of the emission source from the receptor point (the monitoring site). Generally, high wind speed disperses locally emitted pollutants but also brings along pollutants from the upwind areas.

The polar plot (Figure 4, lower panel) shows that high PM_{10} concentrations ($>150 \mu\text{g}/\text{m}^3$) are positively associated with the southwesterly wind with 1–3 m/s speed. This is probably due to the fact that southwesterly wind brings emissions from Taif road and the sandy deserts in this direction. Northeasterly winds with a high wind speed (roughly 3–5 m/s) are also associated with relatively high PM_{10} concentrations (approximately $100\text{--}150 \mu\text{g}/\text{m}^3$).

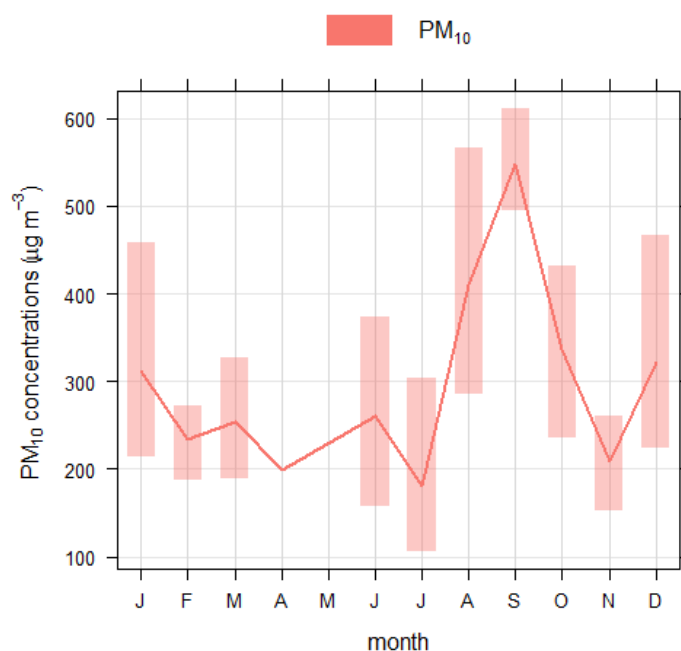


Figure 3. Cont.

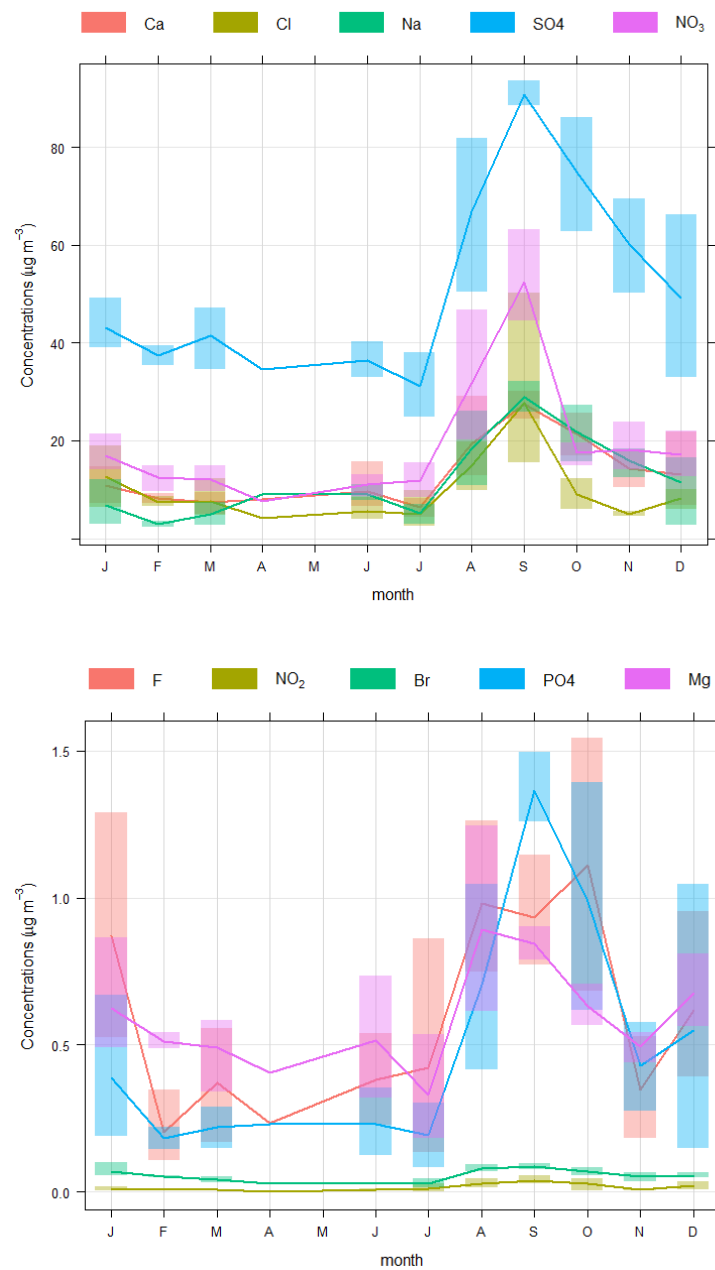


Figure 3. Annual cycles of PM₁₀ (upper panel), major ions, namely Ca, Cl, Na, SO₄, and NO₃ (middle panel), and minor ions, namely F, NO₂, Br, PO₄, and Mg (lower panel) concentrations at Aziziyah site during the study period. In April, data were available only for one week and in May, no data was available, therefore for April, only mean concentration is shown without confident interval and for May, the concentration is not shown at all.

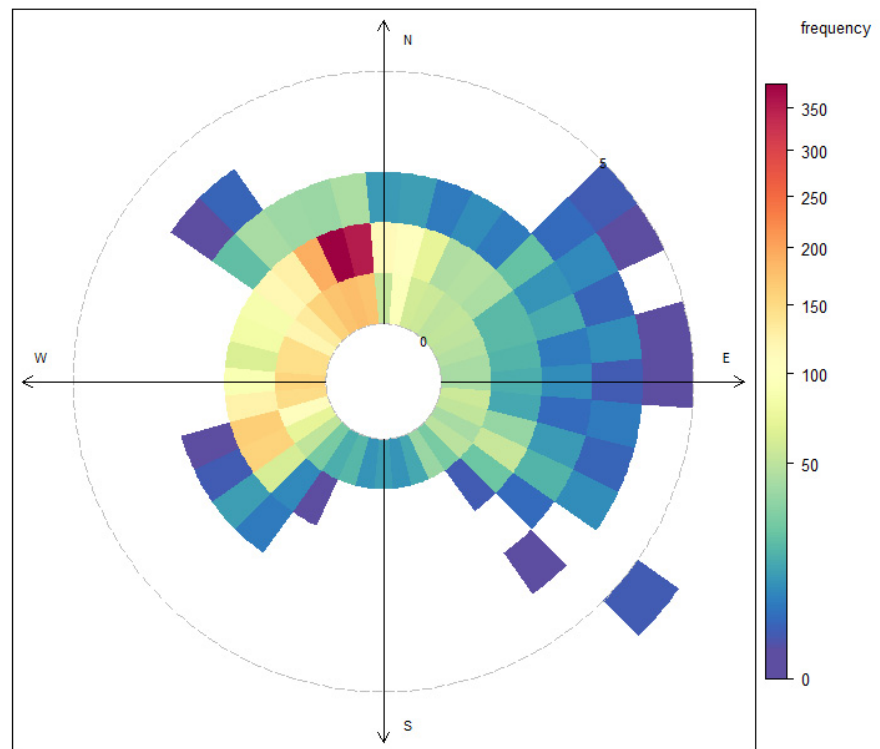
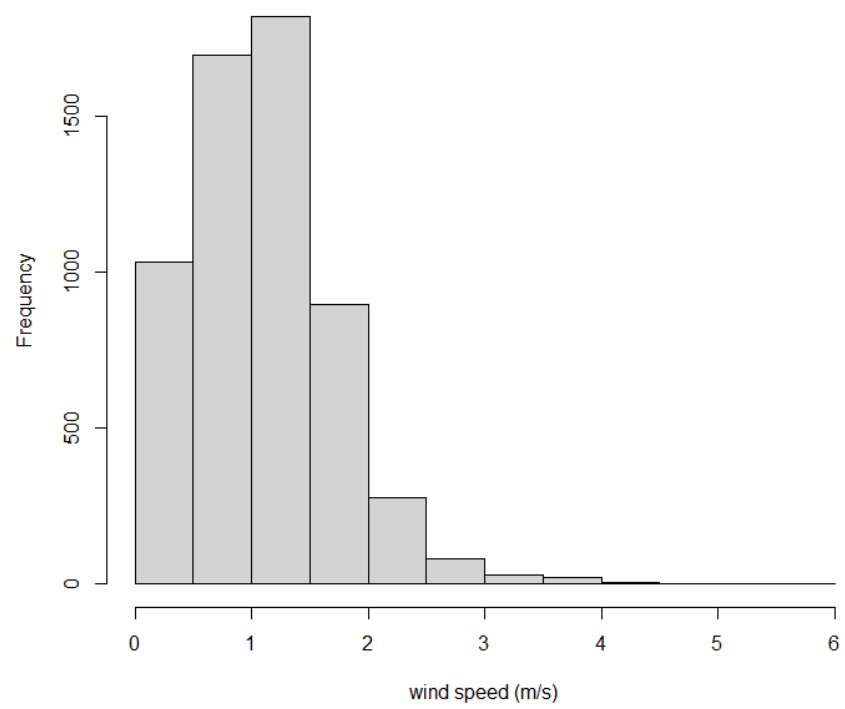


Figure 4. Cont.

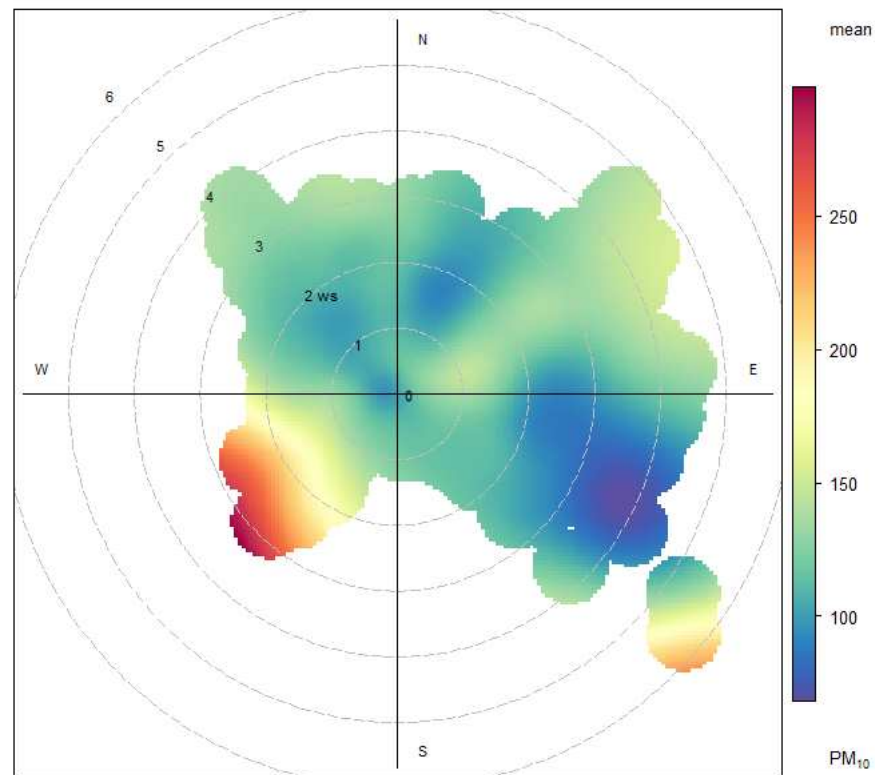


Figure 4. Histogram of wind speed (**upper** panel), polar frequency plot (**middle** panel), and polar plot (**lower** panel) of wind speed and wind direction and PM_{10} , using data from Aziziyah monitoring sites for 2020.

3.1. Correlation Analysis

Correlation analysis was performed to see how different ions correlate with each other and with PM_{10} (Figure 5). Firstly, the data from all sites were pooled into a single table, and then correlation analysis was performed (Figure 5). In addition, correlation analysis was performed for each site separately to see how the correlation varies spatially at different monitoring sites (Figure 5). In pooling the data, this study followed the criteria of Khodeir et al. [14], who also pooled data of particulate matter and its constituents collected at several sites in Jeddah, Saudi Arabia. The purpose of pooling data from several sites is to increase the number of samples in the dataset, which enhance the statistical power of the analysis. Pooling can also help determine the common emission sources of all sites in a city. Correlation plots of individual sites have different shapes and colours probably caused by variations in local emission sources, land-use, geographical conditions, and microclimatic characteristics. The values of correlation coefficients slightly varied at different sites. For example, Abdeyah showed a slightly stronger correlation, whereas Misfalah showed weaker correlations compared to the other sites (Figure 5). Misfalah is located inside Makkah city and continuously remains busy in terms of road traffic, shops, and hotels. In contrast, Abdeyah is located outside Makkah city in the southeast direction in a suburban location. Misfalah is walking distance (about 2 km) from Al-Haram (the Holy Mosque), whereas Abdeyah is situated approximately 16 km from Al-Haram. Therefore, these two sites have totally different emission and dispersion characteristics, which control the levels and composition of air pollution.

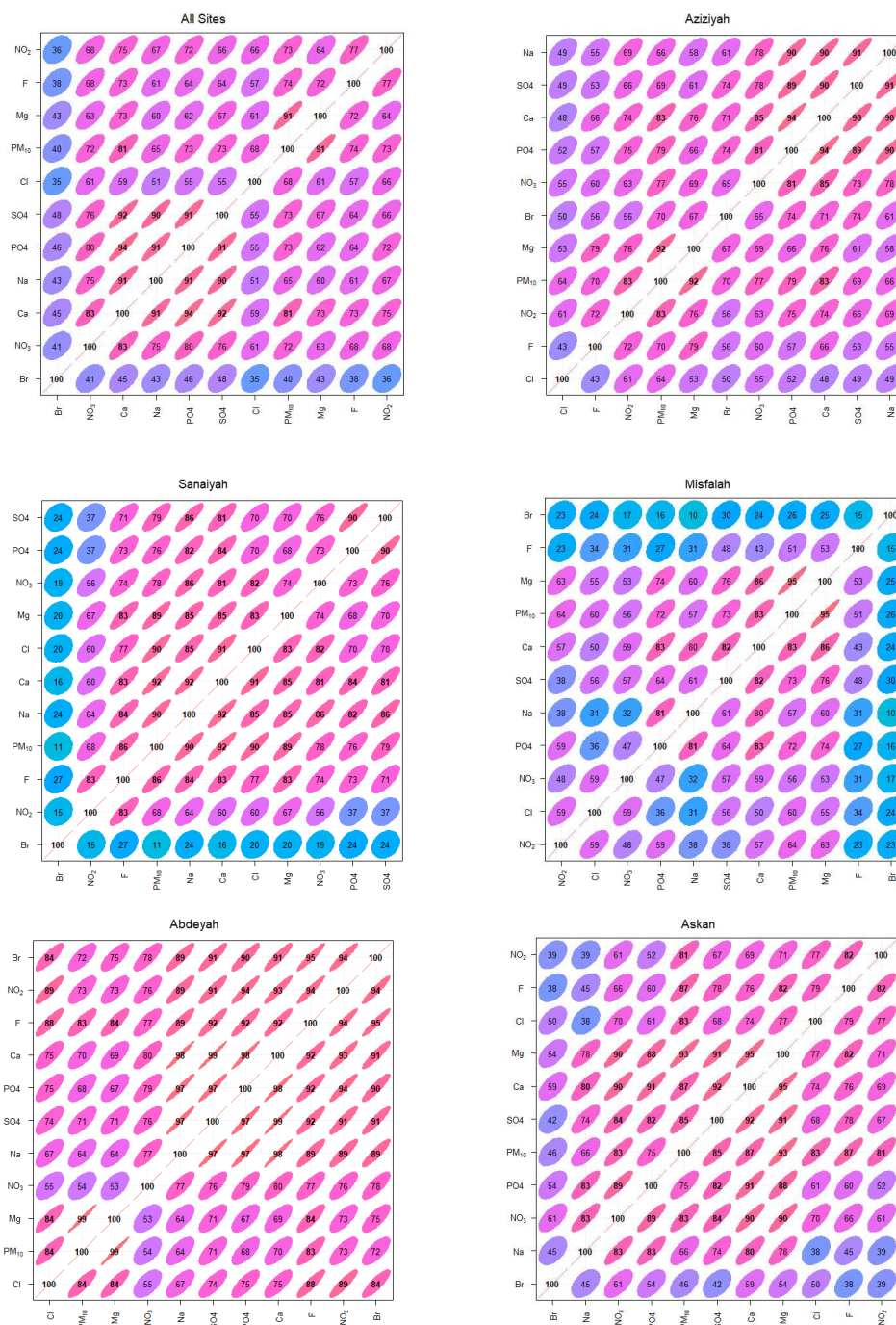


Figure 5. Correlation plots of different ions with each other and with PM₁₀ at each sampling site in Makkah. The top panel “all sites” shows correlation plots of the pooled data from all sites, while the other panels are named according to the name of the sites.

In this study, we followed the methodology of Schober et al. [36], who suggested considering absolute values of the correlation coefficient (*r*) between 0.00 and 0.09 as negligible, between 0.10 and 0.39 as weak, between 0.40 and 0.69 as moderate, between 0.70 and 0.89 as strong, and values 0.90 or greater as a very strong correlation [36]. Figure 5 show that there is no negligible correlation, but there are some weak correlations between different ions. However, most of the correlation coefficients are either moderate, strong, or very strong. When data from all sites were pooled (Figure 5), PM₁₀ had a moderate correlation with Br⁻, Cl⁻ and Na⁺, strong correlation with NO₃⁻, Ca²⁺, SO₄²⁻, PO₄³⁻, F⁻ and NO₂⁻, and a very strong correlation with Mg²⁺. PM₁₀ showed a very strong correlation

with Mg^{2+} at all sites. Br^- and Cl^- showed either weak or moderate correlation with all other ions and PM_{10} . A very strong correlation was also found between SO_4^{2-} vs. Ca^{2+} , SO_4^{2-} vs. Na^+ , SO_4^{2-} vs. PO_4^{3-} , PO_4^{3-} vs. Ca^{2+} , PO_4^{3-} vs. Na^+ , and Na^+ vs. Ca^{2+} . A strong correlation was found between NO_3^- vs. Ca^{2+} , NO_3^- vs. Na^+ , NO_3^- vs. PO_4^{3-} , NO_3^- vs. SO_4^{2-} , Ca^{2+} vs. Mg^{2+} , Ca^{2+} vs. F^- , Ca^{2+} vs. NO_2^- , PO_4^{3-} vs. NO_2^- , Mg^{2+} vs. F^- , and F^- vs. NO_2^- . The correlation coefficient between Cl^- and Na^+ was 0.51 for all sites, 0.49 for Aziziyah, 0.85 for Sanaiyah, 0.31 for Misfalah, 0.67 for Abdeyah, and 0.38 for Askan. Misfalah and Askan have weak, all sites, Aziziyah and Abdeyah have moderate, and Sanaiyah has a strong correlation. This shows that different emission sources contribute to the emission of Na^+ and Cl^- , affecting their correlation at different sites. Researchers have reported that not only the levels of PM_{10} and its constituents but also the correlation between them vary within a city. Kumar et al. [37] reported that levels of F^- , Cl^- , NO_3^- , SO_4^{2-} , Na^+ , NH_4^+ , K^+ , Mg^{2+} , and Ca^{2+} ranged between 0.30–0.37, 4.62–5.30, 0.97–2.12, 11.44–12.23, 3.15–5.67, 3.78–5.84, 2.85–4.44, 0.97–1.08, and 2.73–3.66 $\mu g/m^3$, respectively in Mumbai City, India. They also reported that the correlation between various ions varied at different sites within the same city. Non-sea salt sources (e.g., anthropogenic emission, soil particles and biomass burning) are responsible for different correlations between ions within a city [38,39].

3.2. Principal Component Analysis (PCA)

Results of PCA are shown in Table 3. Here, we selected the first four principal components (PCs) as they explained most of the variance in the data ranging from 84% to 98%. When data were pooled for all sites, PC1 explained the most variations (70%), followed by PC2 (8%), PC3 (7%), and PC4 (4%). The first four PCs explained 89% variations for all sites. It should be noted that PCA analysis was performed on the ionic component of PM only, which ranged from 31.99% to 41.40% of the PM_{10} mass. At Aziziyah, the four PCs explained 91% variance, at Sanaiyah 93%, at Misfalah 84%, at Abdeyah 98%, and at Askan 94%. PC1 explains over 70% variance in the data, except at Misfalah, where PC 1 explains 57% variance. Misfalah site has different data structure compared to the other sites. This is also shown in the correlation plots, where Misfalah demonstrated a weaker correlation between different species than the other sites. Variance and correlation among different species are dependent on the emission sources and factors responsible for the dispersion of the pollutants. Misfalah is located near Al-Haram and continuously remains busy in terms of road traffic and visitors all year round.

Table 3. Principal components and relevant metrics (Eigenvalue, % variance, and % cumulative variance) of each PC.

Metrics	Aziziyah				Sanaiyah			
	PC1	PC2	PC3	PC4	PC1	PC2	PC3	PC4
Eigenvalue	2.82	0.97	0.79	0.68	2.83	0.99	0.94	0.59
% Variance	0.72	0.09	0.06	0.04	0.73	0.09	0.08	0.03
% Cumulative variance	0.72	0.81	0.87	0.91	0.73	0.82	0.90	0.93
Metrics	Misfalah				Abdeyah			
	PC1	PC2	PC3	PC4	PC1	PC2	PC3	PC4
Eigenvalue	2.51	1.06	0.94	0.93	3.03	0.99	0.58	0.52
% Variance	0.57	0.10	0.08	0.08	0.84	0.09	0.03	0.02
% Cumulative variance	0.57	0.68	0.76	0.84	0.84	0.93	0.96	0.98
Metrics	Askan				All Sites			
	PC1	PC2	PC3	PC4	PC1	PC2	PC3	PC4
Eigenvalue	2.87	1.06	0.84	0.50	2.78	0.94	0.86	0.69
% Variance	0.75	0.10	0.06	0.02	0.70	0.08	0.07	0.04
% Cumulative variance	0.75	0.85	0.92	0.94	0.70	0.78	0.85	0.89

PM₁₀ loadings in each PC are shown in Table 4 for the data pooled for all sites, which help us identify the variables (ions) that contribute to each PC. Table 5 show the factor loading of each ion species on the four identified PCs. The four PCs are identified as four major emission sources in the study area, which are:

1. Emissions from road traffic, including exhaust emission, wear-and-tear emissions and resuspension of dust particles on roadsides (F⁻, SO₄²⁻, NO₃⁻, Ca²⁺, Na⁺, Mg²⁺, Br⁻, Cl⁻, NO₂⁻, PO₄³⁻) [40,41].
2. Mineral dust (Cl⁻, F⁻, Na⁺, Ca²⁺, Mg²⁺, PO₄³⁻) [41–43].
3. Industrial and construction–demolition emissions (F⁻, SO₄²⁻, Ca²⁺, Mg²⁺) [42].
4. Seaspray and marine aerosols (Cl⁻, Br⁻, Mg²⁺, Na⁺) [40].

Table 4. Factor loadings for PM₁₀ in different principal components using the pooled data from all sites.

	PC1	PC2	PC3	PC4
Variables contributing positively to each PC	F ⁻ , Cl ⁻ , NO ₂ ⁻ , Br ⁻ , NO ₃ ⁻ , PO ₄ ³⁻ , SO ₄ ²⁻ , Na ⁺ , Ca ²⁺ , Mg ²⁺	Cl ⁻ , F ⁻ , Na ⁺ , Ca ²⁺ , Mg ²⁺ , PO ₄ ³⁻	F ⁻ , SO ₄ ²⁻ , Ca ²⁺ , Mg ²⁺	Cl ⁻ , Br ⁻ , Mg ²⁺ , Na ⁺
Eigenvalue	2.78	0.94	0.86	0.69
% Variance	0.70	0.08	0.07	0.04
% Cumulative variance	0.70	0.78	0.85	0.89

Table 5. Factor loadings of each ion specie on the identified four principal components.

Ions	PC1	PC2	PC3	PC4
F ⁻	-0.31	0.42	-0.13	0.16
Cl ⁻	-0.30	0.40	0.20	-0.63
NO ₂ ⁻	-0.28	0.50	0.00	0.58
Br ⁻	-0.23	-0.17	0.90	0.21
NO ₃ ⁻	-0.34	-0.20	0.03	-0.10
PO ₄ ³⁻	-0.33	-0.29	-0.08	-0.24
SO ₄ ²⁻	-0.34	-0.02	-0.28	-0.02
Na ⁺	-0.29	-0.50	-0.21	0.33
Ca ²⁺	-0.36	-0.09	-0.05	-0.03
Mg ²⁺	-0.36	-0.01	-0.10	-0.10

SO₄²⁻ and NO₃⁻ are the two major ions, which on average contribute 50.25% and 16.43% to the ion concentrations in Makkah (Table 2). NO₃⁻ and SO₄²⁻ are secondary aerosols that are formed in the atmosphere through homogenous gas-phase oxidation of the SO₂ and NO_x, which are emitted by combustion sources, mainly road traffic in urban areas. The contribution of NO₃⁻ and SO₄²⁻ varied slightly at different monitoring sites. The highest contribution of NO₃⁻ was observed at Aziziyah (18.13%), whereas the highest contribution of SO₄²⁻ was observed at the Misfalah site (52.73%). These are both urban traffic sites, and road traffic are the major emission source of traffic-related air pollutants (e.g., NO_x and SO₂). Ca²⁺, Mg²⁺, PO₄³⁻, Cl⁻, and Na⁺ mainly come from mineral dust. Makkah has high levels of background PM₁₀ concentrations, which is blown to the city from the surrounding deserts. These ions also have high loading in the dust on the roadside, which is resuspended to the atmosphere as vehicles pass by. Cl⁻, Br⁻, F⁻, and Na⁺ are found in seaspray but at the same time are found in the soil dust. Sander et al. [40] reported that sea salt is the major source of atmospheric Cl⁻, Br⁻ and Na⁺; however, in arid and semi-arid regions, a strong wind can inject a large amount of soil dust into the atmosphere, which contains a significant amount of these ions. These ions from both sea spray and

soil dust travel long distances and are identified to contribute to the concentrations of the observed ions in Makkah. F^- , B^- , and Cl^- enter the atmosphere from both natural and anthropogenic sources. Natural sources include soil dust, marine aerosols, and volcanic eruptions, whereas the main anthropogenic source is biomass burning [42]. Seawater has Na and Cl in a ratio of 0.56, approximately [44,45], whereas the average ratio of Na and Cl in PM_{10} samples analysed in this study in Makkah was 1.47. This showed that other natural and anthropogenic sources added both Na and Cl disproportionately [38]. Alternatively, we can say that Cl loss has occurred in the atmosphere, which could have been caused by the reaction of acids, such as HNO_3 and H_2SO_4 with NaCl [38]. On a global scale, 82% PO_4^{3-} comes from mineral sources, 12% from biogenic particles, and 5% from combustion sources [46]. However, the proportions vary spatially from region to region, and in urban areas, the contribution of combustion source might be much larger. Ca^{2-} and Mg^{2-} are good markers for crustal dust and can be found in mineral dust, windblown dust, construction and demolition dust, and the resuspension of dust particles [23,47]. Zhang et al. [42] collected PM_{10} samples from soil dust, urban dust, construction dust, coal-fired power plants dust, and steel plant dust were sampled. The characteristic components in their samples were Fe and Ca in urban dust and soil dust, Ca and Mg in construction dust, Fe, Ca^{2+} and SO_4^{2-} in steel dust, and SO_4^{2-} and Ca in power plants dust.

PM_{10} in Makkah is generated by natural sources (e.g., dust storms) as well as anthropogenic sources (e.g., road traffic, power plants, and emission from construction and demolition activities). Therefore, actions are required to cut emissions and manage air quality effectively. Air quality improvement measures may include:

1. Improving the quality of vehicle fleets (e.g., banning old polluting vehicles and retrofitting old vehicles with new technology) [10];
2. Growing more trees in the city, especially on roadsides, which not only control pollution but help moderate temperature [48,49];
3. Implementing an effective water spray programme during construction and demolition activities to reduce the amount of dust [50];
4. Electrifying vehicle fleets and providing charging facilities [51];
5. Discouraging idling [10];
6. Further improving and encouraging public transport [10];
7. Taking action to encourage active mobility, including cycling and walking [52].

4. Conclusions

In this paper, water-soluble cations and anions are analysed in Makkah, Saudi Arabia. PM_{10} samples were collected at five sites from March 2020 to March 2021 and analysed in the laboratory for cations and anions contents. PM_{10} samples were analysed for F^- , Cl^- , NO_2^- , Br^- , NO_3^- , PO_4^{3-} , SO_4^{2-} , Na^+ , Ca^{2+} , and Mg^{2+} . PM_{10} concentrations were quantified at all five sites. PM_{10} concentrations ($\mu g/m^3$) at the Aziziyah site ranged from 82.11 to 739.61, which was the highest for the five sites. At Sanaiyah, the range of PM_{10} concentrations ($\mu g/m^3$) was 65.37 to 421.71, at Misfalah, the range was 25.20 to 466.60, at Abdeyah, the range was 52.56 to 507.23, and at Askan, the range was 40.91 to 471.99. Air quality standards set by the Presidency of Meteorology and Environment (PME) of Saudi Arabia for PM_{10} is 340 ($\mu g/m^3$) for 24 h average and 80 ($\mu g/m^3$) for an annual average. PM_{10} levels exceeded the air quality objectives, which show the seriousness of particle pollution in Makkah. On average, the cations and anions analysed in this study made a 37.81% contribution to the PM_{10} concentrations. The percentage proportion of ions to PM_{10} varied from site to site and ranged from 31.99% (ions—70.28 $\mu g/m^3$ and PM_{10} —219.7 $\mu g/m^3$) at Misfalah to 41.40% (ions—73.69 $\mu g/m^3$ and PM_{10} —177.99 $\mu g/m^3$) at Abdeyah, which were used to determine the emission sources. This means about 58 to 68% of PM_{10} consist of other components, including organic chemicals, metals, and soil or dust particles. On average SO_4^{2-} , NO_3^- , Ca^{2+} , Na^+ , and Cl^- contributed 50.25%, 16.43%, 12.11%, 11.12%, and 8.70%, respectively. The percent contribution of individual ions to the total mass of ions varies from site to site; however, the order is the same for all sites, which

is $\text{SO}_4^{2-} > \text{NO}_3^- > \text{Ca}^{2+} > \text{Na}^+ > \text{Cl}^-$. Principal component analysis was used to identify the main emission sources of PM_{10} in Makkah. Four PCs were identified that explained 89% variations in the data. PC1 explained 70% variability in the data, whereas PC2 to PC4 explained 8%, 7% and 4% variations, respectively. From the PCA results, four major emission sources are identified based on ions concentrations (up to 42% of the PM_{10} mass), which are: (1) Emissions from road traffic, including exhaust emission, wear-and-tear emissions and resuspension of dust particles on roadsides (F^- , SO_4^{2-} , NO_3^- , Ca^{2+} , Na^+ , Mg^{2+} , Br^- , Cl^- , NO_2^- , PO_4^{3-}); (2) Mineral dust (Cl^- , F^- , Na^+ , K^+ , Ca^{2+} , Mg^{2+} , PO_4^{3-}); (3) Industrial and construction-demolition emissions (F^- , SO_4^{2-} , Ca^{2+} , Mg^{2+}); and (4) sea spray and marine aerosols (Cl^- , Br^- , Mg^{2+} , Na^+).

Several compounds, which are part of the PM_{10} , have been reported e.g., [53–55] to be adsorbed on quartz or glass fibre filters including PAH, formaldehydes, and n-butanes, which might affect the levels of PM_{10} and its ionic constituents. The work is still ongoing, and we aim to further analyse the metal contents of the PM_{10} , which will provide a greater insight into the emission sources of PM_{10} .

Author Contributions: Idea initiation, T.M.H., S.M., J.Z. and E.A.M.; PM_{10} sample collection, T.M.H., J.Z. and E.A.M.; sample lab analysis, J.Z.; statistical analysis, T.M.H. and S.M.; writing—first draft T.M.H., S.M. and J.Z.; visualisation, S.M. and T.M.H.; review, T.M.H., S.M., J.Z. and E.A.M. All authors have read and agreed to the published version of the manuscript.

Funding: This project was funded by the King Abdulaziz City of Science and Technology (KACTS) (Research project number 14-ENV2582-10).

Institutional Review Board Statement: Not applicable.

Acknowledgments: We are thankful to King Abdulaziz City of Science and Technology (KACTS) for funding this research project (14-ENV2582-10). The authors are also thankful to the Custodian of the Holy Two Mosques Institute for Hajj and Umrah Research and the Scientific Research Institute at Umm Al-Qura University for their support and assistance.

Conflicts of Interest: The authors declare no conflict of interest.

References

- Dastoorpoor, M.; Sekhavatpour, Z.; Masoumi, K.; Mohammadi, M.J.; Aghababaeian, H.; Khanjani, N.; Hashemzadeh, B.; Vahedian, M. Air pollution and hospital admissions for cardiovascular diseases in Ahvaz, Iran. *Sci. Total Environ.* **2019**, *652*, 1318–1330. [CrossRef]
- WHO. Ambient (Outdoor) Air Pollution. 2018. Available online: [https://www.who.int/news-room/fact-sheets/detail/ambient-\(outdoor\)-air-quality-and-health](https://www.who.int/news-room/fact-sheets/detail/ambient-(outdoor)-air-quality-and-health) (accessed on 5 May 2021).
- World Bank. *The Cost of Air Pollution: Strengthening the Economic Case for Action*; World Bank: Washington, DC, USA, 2016; Available online: <https://openknowledge.worldbank.org/handle/10986/25013> (accessed on 5 November 2021).
- WHO. Air Pollution and Health: Summary. 2006. Available online: <https://www.who.int/airpollution/ambient/about/en/> (accessed on 18 May 2021).
- Power, A.L.; Tennant, R.K.; Jones, R.T.; Tang, Y.; Du, J.; Worsley, A.T.; Love, J. Monitoring Impacts of Urbanisation and Industrialisation on Air Quality in the Anthropocene Using Urban Pond Sediments. *Front. Earth Sci.* **2018**, *6*, 31. [CrossRef]
- Nayebare, S.R.; Aburizaiza, O.S.; Khwaja, H.A.; Siddique, A.; Hussain, M.M.; Zeb, J.; Khatib, F.; Carpenter, D.O.; Blake, D.R. Chemical Characterization and Source Apportionment of $\text{PM}_{2.5}$ in Rabigh, Saudi Arabia. *Aerosol Air Qual. Res.* **2016**, *16*, 3114–3129. [CrossRef]
- Mirza, A.P. Annual Number of Hajj Pilgrims to Saudi Arabia from 1999 to 2019. 2021. Available online: <https://www.statista.com/statistics/617696/saudi-arabia-total-hajj-pilgrims/> (accessed on 12 December 2021).
- Seroji, A.R. Particulates in the atmosphere of Makkah and Mina valley during the Ramadan and Hajj sea-seasons of 2004 and 2005. In *Air Pollution XIX*; WIT Transactions on Ecology and the Environment; WIT Press: Southampton, UK, 2011; Volume 147.
- Munir, S.; Habeebullah, T.M.; Seroji, A.; Morsy, E.A.; Mohammed, A.M.; Abu Saud, W.; Abdou, A.E.; Awad, A.H. Modeling Particulate Matter Concentrations in Makkah, Applying a Statistical Modeling Approach. *Aerosol Air Qual. Res.* **2013**, *13*, 901–910. [CrossRef]
- Simpson, I.J.; Aburizaiza, O.S.; Siddique, A.; Barletta, B.; Blake, N.J.; Gartner, A.; Khwaja, H.; Meinardi, S.; Zeb, J.; Blake, D.R. Air Quality in Mecca and Surrounding Holy Places in Saudi Arabia During Hajj: Initial Survey. *Environ. Sci. Technol.* **2014**, *48*, 8529–8537. [CrossRef]

11. Nayebare, S.R.; Aburizaiza, O.S.; Siddique, A.; Carpenter, D.O.; Hussain, M.M.; Zeb, J.; Aburiziza, A.J.; Khwaja, H.A. Ambient air quality in the holy city of Makkah: A source apportionment with elemental enrichment factors (EFs) and factor analysis (PMF). *Environ. Pollut.* **2018**, *243*, 1791–1801. [[CrossRef](#)] [[PubMed](#)]
12. Cusack, M.; Arrieta, J.M.; Duarte, C.M. Source Apportionment and Elemental Composition of Atmospheric Total Suspended Particulates (TSP) Over the Red Sea Coast of Saudi Arabia. *Earth Syst. Environ.* **2020**, *4*, 777–788. [[CrossRef](#)]
13. Habeebullah, M.T. Chemical Composition of Particulate Matters in Makkah—Focusing on Cations, Anions and Heavy Metals. *Aerosol. Air Qual. Res.* **2016**, *16*, 336–347. [[CrossRef](#)]
14. Khoder, M.; Shamy, M.; Alghamdi, M.; Zhong, M.; Sun, H.; Costa, M.; Chen, L.-C.; Maciejczyk, P. Source apportionment and elemental composition of PM_{2.5} and PM₁₀ in Jeddah City, Saudi Arabia. *Atmos. Pollut. Res.* **2012**, *3*, 331–340. [[CrossRef](#)]
15. Shahsavani, A.; Naddafi, K.; Haghhighifard, N.J.; Mesdaghinia, A.; Yunesian, M.; Nabizadeh, R.; Arhami, M.; Yarahmadi, M.; Sowlat, M.H.; Ghani, M.; et al. Characterization of ionic composition of TSP and PM₁₀ during the Middle Eastern Dust (MED) storms in Ahvaz, Iran. *Environ. Monit. Assess* **2012**, *184*, 6683–6692. [[CrossRef](#)]
16. Pio, C.; Alves, C.; Nunes, T.; Cerqueira, M.; Lucarelli, F.; Nava, S.; Calzolari, G.; Gianelle, V.; Colombi, C.; Amato, F.; et al. Source apportionment of PM_{2.5} and PM₁₀ by Ionic and Mass Balance (IMB) in a traffic-influenced urban atmosphere, in Portugal. *Atmos. Environ.* **2020**, *223*, 117217. [[CrossRef](#)]
17. Bozkurt, Z. Seasonal variation of water-soluble inorganic ions in PM₁₀ in a city of northwestern Turkey. *Environ. Forensics* **2017**, *19*, 1–13. [[CrossRef](#)]
18. Liu, H.; Zheng, J.; Qu, C.; Zhang, J.; Wang, Y.; Zhan, C.; Yao, R.; Cao, J. Characteristics and Source Analysis of Water-Soluble Inorganic Ions in PM₁₀ in a Typical Mining City, Central China. *Atmosphere* **2017**, *8*, 74. [[CrossRef](#)]
19. Deshmukh, D.K.; Tsai, Y.I.; Deb, M.K.; Zarmas, P. Characteristics and sources of water-soluble ionic species associated with PM₁₀ particles in the ambient air of central India. *Bull. Environ. Contam. Toxicol.* **2012**, *89*, 1091–1097. [[CrossRef](#)] [[PubMed](#)]
20. CDSI. Central Department of Statistics and Information of Saudi Arabia. 2020. Available online: <https://www.stats.gov.sa/en> (accessed on 19 September 2021).
21. Almazroui, M. Temperature variability over Saudi Arabia during the period 1978–2010 and its association with global climate indices. *Met. Environ. Arid Land Agric. Sci.* **2012**, *23*, 85–108. [[CrossRef](#)]
22. Ferreira, R.; Nunes, C.; Souza, M.; Canela, M. Multivariate Optimization of Extraction Variables of PAH in Particulate Matter (PM₁₀) in Indoor/Outdoor Air at Campos dos Goytacazes, Brazil. *J. Braz. Chem. Soc.* **2021**, *32*, 618–625. [[CrossRef](#)]
23. Sowlat, M.H.; Naddafi, K.; Yunesian, M.; Jackson, P.L.; Lotfi, S.; Shahsavani, A. PM₁₀ Source Apportionment in Ahvaz, Iran, Using Positive Matrix Factorization | Enhanced Reader. *Clean Soil Air Water* **2013**, *41*, 1143–1151. [[CrossRef](#)]
24. CARB. Standard Operating Procedure for the Determination of PM₁₀ Mass by Gravimetric Analysis. Northern Laboratory Branch, Monitoring and Laboratory Division. 2018. Available online: <https://www.arb.ca.gov/aaqm/sop/mld016.pdf> (accessed on 20 September 2021).
25. R Core Team RC. *R: A Language and Environment for Statistical Computing*; R Foundation for Statistical Computing: Vienna, Austria; Available online: <http://www.r-project.org/index.html> (accessed on 20 April 2021).
26. Carslaw, D. The Openair Manual: Open-Source Tools for Analysing Air Pollution Data. 2019. Available online: <https://davidcarslaw.com/files/openairmanual.pdf> (accessed on 23 April 2021).
27. Wickham, H. *ggplot2: Elegant Graphics for Data Analysis*, 2nd ed.; Springer International Publishing: Berlin/Heidelberg, Germany, 2009; Available online: <https://link.springer.com/book/10.1007/978-0-387-98141-3> (accessed on 12 August 2021).
28. Park, K.; Dam, H.D. Characterization of metal aerosols in PM₁₀ from urban, industrial, and Asian Dust sources. *Environ. Monit. Assess.* **2008**, *160*, 289–300. [[CrossRef](#)] [[PubMed](#)]
29. Zuska, Z.; Kopcinska, J.; Dacewicz, E.; Skowera, B.; Wojkowski, J.; Wojtaszek, A.Z. Application of the Principal Component Analysis (PCA) Method to Assess the Impact of Meteorological Elements on Concentrations of Particulate Matter (PM₁₀): A Case Study of the Mountain Valley (the Sacz Sasin, Poland). *Sustainability* **2019**, *11*, 6740. [[CrossRef](#)]
30. Cesari, D.; Amato, F.; Pandolfi, M.; Alastuey, A.; Querol, X.; Contini, D. An inter-comparison of PM₁₀ source apportionment using PCA and PMF receptor models in three European sites. *Environ. Sci. Pollut. Res.* **2016**, *23*, 15133–15148. [[CrossRef](#)]
31. ArRiyadh Air Quality. Air Quality Standards, Legislations and Policy. Available online: <http://aq.riyadhenv.gov.sa/aq/about-us/riyadh-air-quality-standards/> (accessed on 18 December 2021).
32. Mohammed, A.M.F.; Munir, S.; Habeebullah, T.M. Characterization of atmospheric aerosols in Makkah. *Int. J. Agric. Environ. Res.* **2021**, *1*, 1–17.
33. Al-Jeelani, H.A. Evaluation of air quality in the Holy Makkah during Hajj season 1425 H. *J. Appl. Sci. Res.* **2009**, *5*, 115–121.
34. Othman, N.; Jafri, M.Z.M.; San, L.H. Estimating Particulate Matter Concentration over Arid Region Using Satellite Remote Sensing: A Case Study in Makkah, Saudi Arabia. *Mod. Appl. Sci.* **2010**, *4*, 131. [[CrossRef](#)]
35. Morsy, E.; Habeebullah, T.M.; Othman, A. Assessing the air quality of megacities during the COVID-19 pandemic lockdown: A case study from Makkah City, Saudi Arabia. *Arab. J. Geosci.* **2021**, *14*, 1–12. [[CrossRef](#)]
36. Schober, P.; Boer, C.; Schwarte, L.A. Correlation Coefficients: Appropriate Use and Interpretation. *Anesth. Analg.* **2018**, *126*, 1763–1768. [[CrossRef](#)]
37. Kumar, R.; Elizabeth, A.; Gawane, A.G. Air Quality Profile of Inorganic Ionic Composition of Fine Aerosols at Two Sites in Mumbai City. *Aerosol Sci. Technol.* **2006**, *40*, 477–489. [[CrossRef](#)]

38. Cheng, Z.; Lam, K.; Chan, L.; Wang, T.; Cheng, K. Chemical characteristics of aerosols at coastal station in Hong Kong. I. Seasonal variation of major ions, halogens and mineral dusts between 1995 and 1996. *Atmos. Environ.* **2000**, *34*, 2771–2783. [[CrossRef](#)]
39. Keene, W.C.; Pszenny, A.A.P.; Galloway, J.N.; Hawley, M.E. Sea-salt corrections and interpretation of constituent ratios in marine precipitation. *J. Geophys. Res. Space Phys.* **1986**, *91*, 6647–6658. [[CrossRef](#)]
40. Sander, R.; Keene, W.C.; Pszenny, A.A.P.; Arimoto, R.; Ayers, G.P.; Baboukas, E.; Caine, J.M.; Crutzen, P.J.; Duce, R.A.; Hönninger, G.; et al. Inorganic bromine in the marine boundary layer: A critical review. *Atmos. Chem. Phys. Discuss.* **2003**, *3*, 1301–1336. [[CrossRef](#)]
41. Jayarathne, T.; Stockwell, C.E.; Yokelson, R.; Nakao, S.; Stone, E.A. Emissions of Fine Particle Fluoride from Biomass Burning. *Environ. Sci. Technol.* **2014**, *48*, 12636–12644. [[CrossRef](#)]
42. Zhang, G.; Ding, C.; Jiang, X.; Pan, G.; Wei, X.; Sun, Y. Chemical Compositions and Sources Contribution of Atmospheric Particles at a Typical Steel Industrial Urban Site. *Sci. Rep.* **2020**, *10*, 7654. [[CrossRef](#)]
43. Chen, L.; Peng, C.; Gu, W.; Fu, H.; Jian, X.; Zhang, H.; Zhang, G.; Zhu, J.; Wang, X.; Tang, M. On mineral dust aerosol hygroscopicity. *Atmos. Chem. Phys. Discuss.* **2020**, *20*, 13611–13626. [[CrossRef](#)]
44. Duxbury, A.C.; Byrne, R.H.; Mackenzie, F.T. Sewater. 2020. Available online: <https://www.britannica.com/science/seawater> (accessed on 12 December 2021).
45. Moller, D. The Na/Cl ratio in rainwater and the seasalt chloride cycle. *Tellus* **1990**, *42*, 254–262. [[CrossRef](#)]
46. Mahowald, N.; Jickells, T.D.; Baker, A.R.; Artaxo, P.; Benitez-Nelson, C.R.; Bergametti, G.; Bond, T.C.; Chen, Y.; Cohen, D.D.; Herut, B.; et al. Global distribution of atmospheric phosphorus sources, concentrations and deposition rates, and anthropogenic impacts. *Glob. Biogeochem. Cycles* **2008**, *22*, 1–19. [[CrossRef](#)]
47. Alleman, L.; Lamaison, L.; Perdrix, E.; Robache, A.; Galloo, J.-C. PM₁₀ metal concentrations and source identification using positive matrix factorization and wind sectoring in a French industrial zone. *Atmos. Res.* **2010**, *96*, 612–625. [[CrossRef](#)]
48. Letter, C.; Jäger, G. Simulating the potential of trees to reduce particulate matter pollution in urban areas throughout the year. *Environ. Dev. Sustain.* **2019**, *22*, 4311–4321. [[CrossRef](#)]
49. Chen, L.; Liu, C.; Zhang, L.; Zou, R.; Zhang, Z. Variation in Tree Species Ability to Capture and Retain Air-borne Fine Particulate Matter (PM_{2.5}). *Sci. Rep.* **2017**, *7*, 32006.
50. Munir, S.; Habeebullah, T.M.; Seroji, A.R.; Gabr, S.S.; Mohammed, A.M.; Morsy, E.A. Quantifying temporal trends of atmospheric pollutants in Makkah (1997–2012). *Atmos. Environ.* **2013**, *77*, 647–655. [[CrossRef](#)]
51. Barisione, M. Electric Vehicles and Air Pollution: The Claims and The Facts. Clean Air-Analysis & Opinion. 2021. Available online: <https://epha.org/electric-vehicles-and-air-pollution-the-claims-and-the-facts/> (accessed on 18 December 2021).
52. Carnevale, C.; DeAngelis, E.; Finzi, G.; Turrini, E.; Volta, M. Evaluating economic and health impacts of active mobility through an integrated assessment model. *IFAC-PapersOnLine* **2018**, *51*, 49–54. [[CrossRef](#)]
53. Hart, K.M.; Pankow, J.F. Comparison of n-alkane and PAH concentrations collected on quartz fiber and Teflon membrane filters in an urban environment. *J. Aerosol Sci.* **1990**, *21* (Suppl. S1), S377–S380. [[CrossRef](#)]
54. Ligocki, M.P.; Pankow, J.F. Measurements of the gas/particle distributions of atmospheric organic compounds. *Environ. Sci. Technol.* **1989**, *23*, 75–83. [[CrossRef](#)]
55. Klippel, W.; Warneck, P. The formaldehyde content of the atmospheric aerosol. *Atmos. Environ.* **1980**, *14*, 809–818. [[CrossRef](#)]